End13p/Vps4p is required for efficient transport from early to late endosomes in *Saccharomyces cerevisiae*

Regina Zahn[1,§], Brian J. Stevenson[2,§,*], Stephan Schröder-Köhne[2,‡], Bettina Zanolari[2], Howard Riezman[2] and Alan L. Munn[1,¶]

[1]Institute of Molecular Agrobiology, 1 Research Link, National University of Singapore, Singapore, 117604, Republic of Singapore
[2]Biozentrum of the University of Basel, Klingelbergstrasse 70, Basel, CH-4056, Switzerland

*Present address: LICR Office of Information Technology, Ch. des Boveresses 155, CH-1066 Epalinges, Switzerland
‡Present address: BioMedTec Franken e.V., Versbacher Strasse 5, D-97078 Würzburg, Germany
§These authors contributed equally to this work
¶Author for correspondence (e-mail: alan@ima.org.sg)

Accepted 21 February 2001
Journal of Cell Science 114, 1935-1947 © The Company of Biologists Ltd

SUMMARY

end13-1 **was isolated in a screen for endocytosis mutants and has been shown to have a post-internalisation defect in endocytic transport as well as a defect in vacuolar protein sorting (Vps$^-$ phenotype), leading to secretion of newly synthesised vacuolar proteins. Here we demonstrate that *END13* is identical to *VPS4*, encoding an AAA (ATPase associated with a variety of cellular activities)-family ATPase. We also report that the *end13-1* mutation is a serine 335 to phenylalanine substitution in the AAA-ATPase domain of End13p/Vps4p. It has been reported that mutant cells lacking End13p/Vps4p (*end13*(*vps4*)*Δ*) accumulate endocytosed marker dyes, plasma membrane receptors and newly synthesised vacuolar hydrolase precursors in an endosomal compartment adjacent to the vacuole (prevacuolar compartment, or PVC). We find, however, that the *end13* mutants have defects in transport of endocytosed fluorescent dyes, plasma membrane receptors and ligands from small peripherally located early endosomes to larger late endosomes, which are often located adjacent to the vacuole. Our results indicate that End13p/Vps4p may play an important role in multiple steps of membrane traffic through the endocytic pathway.**

Key words: Alpha-factor receptor, Endocytosis, PVC, Vacuolar protein sorting

INTRODUCTION

In *Saccharomyces cerevisiae*, extracellular and plasma membrane materials internalised by endocytosis are transported via at least two endosomal compartments to the vacuole (analogous to the mammalian lysosome), where the internalised material is degraded by resident hydrolases. The endosomal compartments, which were initially defined as early and late endosomes based on the kinetics of cargo delivery, can also be distinguished on the basis of both their characteristic morphology and their density. Early endosomes are smaller, more tubular, of higher density, and are located at the periphery of the cell, whereas late endosomes are larger, multivesicular in appearance, of lighter density, and are located more within the cell and often near the vacuole (Singer and Riezman, 1990; Singer-Krüger et al., 1993; Hicke et al., 1997; Prescianotto-Baschong and Riezman, 1998; reviewed in Munn, 2000).

We have isolated mutants that are blocked at various steps of the endocytic pathway to the vacuole (*end*) using a screen for synthetic lethality with a deletion of the *VMA2*/*VAT2* gene encoding the 60 kDa subunit of the vacuolar H^+-ATPase (*vma2*/*vat2*)*Δ*. A subset of these *end* mutants are competent for receptor-mediated internalisation of radiolabelled ligands at the plasma membrane, but are delayed or blocked at a post-internalisation step in delivery of the ligands to the vacuole. One of these mutants is *end13-1* (Munn and Riezman, 1994; Riezman et al., 1996). In previous work we showed that *end13-1* mutants secrete vacuolar hydrolase precursors into the medium (i.e. they have a vacuolar protein sorting, or Vps$^-$, phenotype) (Munn and Riezman, 1994).

Vacuolar hydrolases in *S. cerevisiae* are delivered to the vacuole via the early secretory pathway (Stevens et al., 1982). They are sorted away from secretory proteins destined for the cell surface upon exit from a late Golgi compartment and are transferred via a distinct set of vesicles to an endosomal prevacuolar compartment (PVC) and then from there to the vacuole (reviewed in Klionsky et al., 1990; Bryant and Stevens, 1998; Munn, 2000). *vps* mutants, which are defective in delivery of newly synthesised soluble vacuolar hydrolases to the vacuole, have been isolated by several laboratories. These mutants have defects in either a late Golgi compartment, in a PVC, in a late endosome or in the vacuole itself and, as a consequence, secrete Golgi-modified precursors of soluble vacuolar hydrolases into the extracellular medium (Bankaitis et al., 1986; Robinson et al., 1988; Rothman and Stevens, 1986; Rothman et al., 1989). The *vps* mutants have been classified into groups A-F based on the morphology of their endosomal and vacuolar compartments and the localisation of the vacuolar H^+-ATPase 60 kDa subunit (Vma2p/Vat2p) (Banta et al., 1988; Raymond et al., 1992). Of these, the class E *vps* mutants exhibit an abnormally enlarged and multilamellar PVC (known as the 'class E compartment'), which accumulates newly synthesised precursors of vacuolar hydrolases as well as endocytosed plasma membrane proteins and Golgi-resident proteins (which

normally recycle to the Golgi from endosomes) (Davis et al., 1993; Piper et al., 1995; Cereghino et al., 1995; Rieder et al., 1996; Babst et al., 1998; Odorizzi et al., 1998).

We show here that *END13* is identical to *VPS4*, a class E *VPS* gene encoding an AAA-family ATPase, which is thought to function in a nucleotide-dependent cycle of binding and release to regulate interaction of other class E *VPS* gene products (Vps24p and Vps32p/Snf7p) with the surface of the PVC (Riezman et al., 1996; Babst et al., 1997; Finken-Eigen et al., 1997; Babst et al., 1998). We characterise the mutation in *end13-1* as an S335F mutation in the AAA-domain and demonstrate that in *end13-1* and *end13Δ* mutants, transport of internalised fluorescent dyes, plasma membrane receptors and ligands from early endosomes to late endosomes is dramatically delayed.

MATERIALS AND METHODS

Media, reagents, strains and plasmids

Saccharomyces cerevisiae strains are listed in Table 1. YPUAD contained 1% yeast extract (Gibco-BRL/Life Technologies, Paisley, UK), 2% peptone (Gibco) and 2% glucose and was supplemented with 40 mg adenine and 20 mg uracil per litre. SD minimal medium was as described (Dulic et al., 1991). All solid growth media contained 2% Bactoagar (Difco, Detroit, MI, USA). Plasmids used are shown in Table 2. Lucifer Yellow carbohydrazide (LY) was the dilithium salt and was obtained from Fluka AG (Buchs, Switzerland). FM4-64 was obtained from Molecular Probes (Eugene, OR, USA). ^{35}S-α-factor was purified from metabolically labelled *MAT*α cell culture supernatants as described (Munn and Riezman, 1994). Recombinant lyticase was prepared as previously described (Hicke et al., 1997). Zymolyase 20T was from US Biologicals (Swampscott, MA, USA). The polyclonal CPY and affinity-purified Ste2p antisera were described previously (Hicke and Riezman, 1996). Monoclonal CPY antibody was from Molecular Probes. Cy3-conjugated anti-rabbit IgG and horseradish peroxidase-conjugated goat anti-mouse IgG and goat anti-rabbit IgG were from Jackson ImmunoResearch Labs (West Grove, PA, USA). Nycodenz (5-(N-2,3-dihydroxypropylacet-amido)-2,4,6-triiodo-N,N′-bis(2,3-dihydroxy-propyl)-isophthalamide), aprotinin, leupeptin, pepstatin A and phenylmethylsulphonylfluoride (PMSF) were from Sigma (St Louis, MO, USA).

Genetic techniques

Mating, sporulation and tetrad analysis were performed as described in Adams et al. (Adams et al., 1997). Transformation of yeast with plasmid DNA was by a modification of the lithium acetate protocol (Munn et al., 1995). Genomic DNA was prepared from *S. cerevisiae* essentially as described by Adams et al. (Adams et al., 1997) and polymerase chain reaction (PCR) amplification was carried out with *Pfu* polymerase (Stratagene, La Jolla, CA, USA). Plasmid DNA was isolated from *S. cerevisiae* using the method of Ward (Ward, 1990).

Cloning of the *END13* locus

end13-1-complementing DNA fragments were obtained by transforming *S. cerevisiae* genomic libraries carried in either the *LEU2*-marked centromere vector YCplac111 (Gietz and Sugino, 1988) (library constructed by Fatima Cvrckova, Institute of Molecular Pathology, Vienna, Austria) or the *URA3*-marked 2μ vector YEp24 (Botstein et al., 1979) (library constructed by M. Carlson, Department of Genetics and Development, Columbia University, New York, USA) into the *end13-1* mutant strain RH2604. Transformants that displayed improved growth at 37°C were retained. Plasmids were recovered, amplified in *E. coli*, and reintroduced into the *end13-1* strain. Three library plasmids were still able to correct the temperature-sensitive growth defect of *end13-1* upon retransformation (pEND13.1 from the YCplac111 library, and pEND13.2 and pEND13.3 from the YEp24 library). The three library plasmids had inserts containing a common 1.8 kb *Hin*dIII fragment and this fragment alone was able to restore normal growth at 37°C to *end13-1*. This insert was sequenced and found to contain a single open reading frame of 437 codons encoding a putative AAA (ATPase associated with a variety of cellular activities)-family ATPase (reviewed in Riezman et al., 1996; sequence submitted to GenBank, accession no. X92680).

To show that the cloned DNA represents the chromosomal locus affected by the *end13-1* mutation, integrative mapping of the cloned locus was performed. The insert in pEND13.1 was subcloned into the *URA3*-tagged integration plasmid YIplac211 (Gietz and Sugino, 1988) to create YIpEND13. This *URA3*-tagged construct was integrated at the chromosomal locus corresponding to the cloned DNA in a wild-type *ura3* haploid strain (RH1800). The resulting strain (RH2902) has *URA3* tightly linked to the cloned wild-type locus. RH2902 was crossed to the *end13-1 ura3* strain RH2605 and the diploid obtained (RH2903) was subjected to tetrad analysis. Of the haploid segregants recovered from this cross, all Ura$^-$ haploids were temperature-sensitive (*end13-1*) and all Ura$^+$ haploids were temperature-resistant (*END13*), indicating that the cloned *URA3*-tagged locus is tightly linked to the original *end13-1* mutation.

Deletion of *END13*

To make an *END13* deletion construct, the insert DNA from pEND13.1 was subcloned into pGEM-4Z (Promega, Madison, WI, USA) and then the 1.1 kb *Acc*I to *Bgl*II fragment (within the complementing *Hin*dIII fragment) was removed and replaced with a 1.1 kb *Hin*dIII fragment carrying the *URA3* gene to create pend13Δ::URA3. This construct has the sequences encoding residues 30-399 of the 437 residues in End13p deleted and replaced with *URA3*. pend13Δ::URA3 was digested with *Sph*I (cuts in insert) and

Table 1. Genotypes of yeast strains used in this study

Strain	Genotype	Source
RH978	*MAT***a** *his4 leu2 ura3 trp1::URA3 bar1*	Riezman laboratory strain
RH1201	*MAT***a**/*MAT*α *his4*/*his4 leu2*/*leu2 ura3*/*ura3 lys2*/*lys2 bar1*/*bar1*	Riezman laboratory strain
RH1800	*MAT***a** *his4 leu2 ura3 bar1*	Riezman laboratory strain
RH2604	*MAT***a** *end13-1 his4 leu2 ura3 bar1* (*lys2*/*LYS2* and *ade6*/*ADE6* not scored)	Munn and Riezman, 1994
RH2605	*MAT*α *end13-1 his4 leu2 ura3 bar1* (*lys2*/*LYS2* and *ade6*/*ADE6* not scored)	Munn and Riezman, 1994
RH2606	*MAT***a** *end13-1 his4 leu2 ura3 trp1::URA3 bar1* (*lys2*/*LYS2* not scored)	Munn and Riezman, 1994
RH2635	*MAT*α *his4 leu2 ura3 bar1*	Riezman laboratory strain
RH2902	*MAT***a** *END13::URA3 his4 leu2 ura3 bar1*	This study
RH2903	*MAT***a**/*MAT*α *END13::URA3*/*end13-1 his4*/*his4 leu2*/*leu2 ura3*/*ura3 lys2*?/*LYS2 ade6*?/*ADE6 bar1*/*bar1*	This study
RH2905	*MAT***a**/*MAT*α *end13-Δ::URA3*/*END13 his4*/*his4 leu2*/*leu2 ura3*/*ura3 lys2*/*lys2 bar1*/*bar1*	This study
RH2906	*MAT***a** *end13-Δ::URA3 his4 leu2 ura3 lys2 bar1*	This study
RH2907	*MAT*α *end13-Δ::URA3 his4 leu2 ura3 lys2 bar1*	This study
SF838-1D *vpl4-1*	*MAT*α *vpl* (*vps*)*4-1 his4 leu2 ura3 ade6 pep4*	Raymond et al., 1992

Table 2. Plasmids used in this study

Plasmid	Description	Source
pEND13.1	Original library clone of *END13* in YCplac111	This study
pEND13.2	Original library clone of *END13* in YEp24	This study
pEND13.3	Original library clone of *END13* in YEp24	This study
YIpEND13	YIplac211 with a 1.8 kb *Hin*dIII fragment carrying *END13*	This study
pGEM-4Z-END13	pGEM-4Z with a 1.8 kb *Hin*dIII fragment carrying *END13*	This study
pend13Δ	pGEM-4Z-END13 in which the 1.1 kb *Acc*I to *Bgl*II fragment of *END13* is replaced by a 1.1 kb *Hin*dIII fragment carrying *URA3*	This study

*Sac*I (cuts in polylinker) to release a fragment containing the *URA3* gene with *END13* flanking sequences. This *URA3* fragment was transformed into the wild-type diploid strain RH1201 and Ura$^+$ transformants were selected on SD medium. One such transformant (RH2905) was subjected to tetrad analysis. Recombinant haploids were scored for Ura$^+$/Ura$^-$ and temperature-sensitive growth. All Ura$^+$ (*end13Δ*) haploids exhibited a temperature-sensitive growth phenotype, while no Ura$^-$ (*END13*) haploids exhibited this phenotype. *MAT***a** and *MAT*α *end13Δ* haploid isolates (RH2906 and RH2907, respectively) were retained for further analysis.

Characterisation of the *end13-1* mutation

To identify the *end13-1* mutation, the *END13* locus was amplified by PCR from genomic DNA prepared from wild-type (RH1800) and *end13-1* mutant (RH2604) cells. The PCR products were subjected to DNA sequence analysis. Two PCR fragments obtained from independent amplifications from *end13-1* were found to have TCC to TTC base transitions in codon 335 of *END13* compared to the wild-type locus.

Fluid-phase endocytosis assays

Fluid-phase endocytosis was measured by uptake and vacuolar accumulation of the membrane-impermeant fluorescent dye Lucifer Yellow carbohydrazide (LY). Cells were grown in YPUAD at 24°C to 0.75-1×10^7 cells/ml, concentrated to 1×10^8 cells/ml in YPUAD containing 5 mg/ml LY, and incubated for 1 hour at 30°C. Cells were then washed and examined microscopically for vacuolar LY as described (Munn and Riezman, 1994), except that the cells were not mounted in agarose.

FM4-64 endocytosis assays

Endocytosis of plasma membrane was assayed by uptake and vacuolar membrane accumulation of the lipid-soluble styryl dye FM4-64 (Vida and Emr, 1995). Cells were grown in YPUAD at 24°C to 0.75-1×10^7 cells/ml. Culture containing 5×10^8 cells was chilled and the cells were harvested. Cells were then resuspended in 50 ml ice-cold YPUAD and FM4-64 was added to a final concentration of 2 mM. The cells were then incubated at 15°C for 20 minutes. A sample of cells was taken (0 minutes) and membrane transport was stopped by addition of sodium azide and sodium fluoride to 12 mM each and chilling on ice. The remaining cells were then washed in ice-cold YPUAD to remove cell-surface FM4-64, resuspended in YPUAD prewarmed to 30°C, and a second sample of cells was taken and treated as described above (0 minute wash). The remainder of the cells was incubated at 30°C and at 5, 10, 15 and 30 minutes after shift samples of cells were taken and treated as described above. Each sample of cells was washed twice in 50 mM sodium phosphate buffer, pH 7, containing 10 mM each of sodium azide and sodium fluoride and viewed in a fluorescence microscope using Texas Red light filters to visualise FM4-64.

Assay for vacuolar degradation of internalised ^{35}S-α-factor

Transport of internalised α-factor to the vacuole was measured by ^{35}S-α-factor degradation assays, which were performed using the pulse-chase protocol (Dulic et al., 1991). Cells were grown in YPUAD at 24°C to 0.75-1.0×10^7 cells/ml and then 1×10^9 cells were harvested and resuspended in ice-cold YPUAD medium. ^{35}S-labelled α-factor (approximately 2-5×10^5 c.p.m.) was allowed to prebind to the cells on ice for 50 minutes. Cells were washed at 4°C to remove unbound ^{35}S-α-factor, and then resuspended in prewarmed 30°C YPUAD medium. The cells were then incubated at 30°C for internalisation of the surface-bound ^{35}S-α-factor and subsequent transport to the vacuole. Samples were taken in duplicate at various time points and processed as described in Dulic et al. (Dulic et al., 1991). Intact and degraded forms of ^{35}S-α-factor in the cell extracts were separated by thin-layer chromatography on Silica gel 60 plates (Merck, Darmstadt, Germany), and visualised by fluorography (Dulic et al., 1991).

Carboxypeptidase Y missorting test

Missorting of the soluble vacuolar protease carboxypeptidase Y (CPY) to the cell surface was examined using a colony immunoblotting assay based on that described by Rothman et al. (Rothman et al., 1986). Cells to be tested were grown on YPUAD solid medium at 24°C in contact with a nitrocellulose filter (Protran BA85, 0.45 μm, Schleicher and Schuell, Dassel, Germany) for 2 days before elution of the cells from the filter. The filters were immunoblotted for secreted CPY using a CPY-specific polyclonal rabbit antiserum and horse radish peroxidase-conjugated goat antirabbit IgG secondary antiserum, and enhanced chemiluminescent detection as described (Munn et al., 1999).

Equilibrium density gradient analysis

Cells were grown in YPUAD at 24°C to 0.75-1×10^7 cells/ml and harvested. For each time point, approximately 1.3×10^7 cells were resuspended in 0.3-0.4 ml YPUAD, cooled to 0°C, and 3-4×10^5 c.p.m. of ^{35}S-α-factor were added. Samples were left on ice for 45 minutes for ^{35}S-α-factor binding. Cells were pelleted to remove unbound ^{35}S-α-factor and resuspended in the same volume of ice-cold YPUAD. A 0 minute sample was taken and sodium azide and sodium fluoride were added to 20 mM. The remaining cells were then shifted to 30°C and samples were taken at various time points of chase and sodium azide and sodium fluoride were added as above. Then the samples were processed as follows in the continual presence of 20 mM each sodium azide and sodium fluoride: cells from each time point were pelleted, treated with reducing agent (cysteamine solution) (Singer and Riezman, 1990), repelleted, and spheroplasted in 400 μl of medium containing 0.6 M sorbitol with an amount of recombinant lyticase sufficient to result in complete spheroplasting after 30-45 minutes at 30°C. Cells were then lysed osmotically by addition of 400 μl of water and the lysate was cleared by centrifugation at 7,500 ***g*** for 5 minutes to yield pellet P1 and supernatant S1. S1 was then subjected to centrifugation in a TL-100 table-top ultracentrifuge (Beckman Instruments, Palo Alto, CA, USA) at 128,000 ***g*** for 30 minutes to yield pellet P2 and supernatant S2. S2 and P1 were immunoblotted for the presence of the cytosolic marker hexokinase to assess the efficiency of lysis, which was 84-97% in each experiment. We therefore did not correct the ^{35}S-α-factor counts obtained from the subsequent gradient analysis for lysis efficiency. Equilibrium density gradient centrifugation was performed on P2 using Nycodenz as described in Singer and Riezman (Singer and Riezman, 1990). Fractions (15) of 650 μl each were collected from the top of the gradient. ^{35}S-α-factor in the various gradient fractions was quantified by counting in a

scintillation counter and the distribution in the gradient was plotted as a function of fraction number.

For analysis of CPY distribution in the gradients, wild-type (RH1800) and *end13-1* (RH2604) cells were grown in YPUAD at 24°C to 1×10^7 cells/ml and 250 OD_{600} units of cells were harvested, spheroplasted and lysed as described above, except that Zymolyase 20T was used for spheroplasting and protease inhibitors were included in the lysis buffer (10 μg/ml aprotinin, 5 μg/ml leupeptin, 16 μg/ml pepstatin A, 1 mM phenylmethylsulphonyl fluoride). After an initial spin at 300 ***g*** for 5 minutes to sediment unlysed cells, P1 and P2 fractions were prepared as above. The P2 fraction was then subjected to equilibrium density gradient centrifugation using the same density gradient and centrifugation conditions used for analysing ^{35}S-α-factor distribution. Fractions (15) of 650 μl each were collected from the top and the protein in each was precipitated with trichloroacetic acid (TCA). TCA precipitates were sedimented, washed in acetone, air dried and dissolved by heating in Laemmli sample buffer. Fractions were then analysed by electrophoresis on 7% SDS-PAGE gels followed by transfer to a polyvinylidene fluoride membrane (Immobilon-P^{SQ}, Millipore, Bedford, MA, USA) and immunoblotting with a CPY-specific monoclonal antiserum using standard procedures (Sambrook et al., 1989). Immunoreactive bands were detected using a horseradish peroxidase-conjugated goat anti-mouse IgG secondary antiserum and enhanced chemiluminescence. The monoclonal CPY-specific antiserum showed no cross-reactivity because no band was detected when extracts of *prc1Δ* cells (deficient in CPY) were immunoblotted (data not shown).

Ste2p endocytosis assays

Cells were grown in YPUAD at 24°C to 0.75-1×10^7 cells/ml and then harvested and resuspended in 50 ml YPUAD to 1×10^7 cells/ml. Cycloheximide was added to 20 μg/ml final concentration to block further Ste2p synthesis and the cells were incubated at 30°C for 10 minutes to chase newly synthesised Ste2p to the plasma membrane. After this incubation, a 0 minute sample (10 ml) was taken and potassium phosphate buffer, pH 6.5, and formaldehyde were added to 100 mM and 3.7%, respectively. The sample was left at room temperature for 2 hours for fixation. Meanwhile, synthetic (non-radioactive) α-factor was added to 1×10^{-7}M final concentration to the remaining culture and the cells were incubated with shaking at 30°C for Ste2p endocytosis. At 8, 16 and 30 minutes after addition of α-factor, further 10 ml samples were taken and fixed as above. Cells were harvested, washed 3× in 10 ml SP (1.2 M sorbitol, 100 mM potassium phosphate buffer, pH 6.5), and resuspended in 1 ml SP containing 20 mM β-mercaptoethanol and 10-15 μl recombinant lyticase. Samples were incubated for 1 hour at 30°C for spheroplasting. Spheroplasts were harvested, washed once with 3 ml SP, and resuspended in 0.25 ml SP. Fixed cells were applied to a poly-L-lysine-treated microscope slide and Ste2p was visualised by indirect immunofluorescence using a polyclonal Ste2p-specific antibody and a Cy3-labelled anti-rabbit IgG secondary antibody.

Fluorescence microscopy

All microscopy was performed using a Zeiss Axiophot (Zeiss, Oberkochen, Germany) or a Leica DMLB (Leica Pte. Ltd., Singapore) microscope fitted with differential interference contrast (Nomarski) and appropriate fluorescence light filters.

RESULTS

Identification of the wild-type *END13* gene

The wild-type *END13* gene was isolated from yeast genomic libraries as described in Materials and Methods. That this cloned DNA represents the locus affected by the *end13-1* mutation was confirmed by integrative mapping of the cloned DNA with *end13-1*. The *END13* open reading frame was found to encode a member of the AAA (ATPase associated with a variety of cellular activities)-family of ATPases, which includes proteins such as Sec18p, Pex6p/Pas8p and Cdc48p (Riezman et al., 1996; Babst et al., 1997; Finken-Eigen et al., 1997). The same gene that we identified as *END13* has also been reported as *VPS4* (Babst et al., 1997). *end13-1* has a vacuolar protein sorting (Vps$^-$) defect (Munn and Riezman, 1994). This defect is partially dominant because *end13-1*/*END13* heterozygous diploids exhibit a defect in vacuolar protein sorting which is intermediate in severity between those observed in wild-type strains and in mutant haploids and homozygous mutant diploids (Fig. 1). Introduction of a centromere-based plasmid containing the wild-type *END13* gene into *end13-1* mutant cells (RH2604) restored growth at 40°C (Fig. 2A), fluid-phase endocytosis of LY (Fig. 2B), and partially corrected the vacuolar protein sorting defect (Fig. 2C).

When an *end13-1* mutant (RH2606) was tested for the ability to complement the Vps$^-$ defect of a *vps4-1* (previously *vpl4-1*) mutant (Raymond et al., 1992), we observed no complementation (Fig. 1). Furthermore, a strain containing a *URA3*-tagged wild-type *END13* locus was crossed to a *vps4-1* mutant and in this cross we found tight genetic linkage between the *URA3* tag and the *vps4-1* mutation (data not shown). Finally, we sequenced the *END13*/*VPS4* locus from an *end13-1* mutant and found a mutation at codon 335. This mutation would result in a change of serine to phenylalanine in the protein product (S335F) (Fig. 3). Together, these results are consistent with *END13* being allelic to *VPS4*.

Loss of End13p causes defects in growth and endocytosis similar to those of *end13-1* mutants

We deleted the *END13* gene in a wild-type diploid strain to

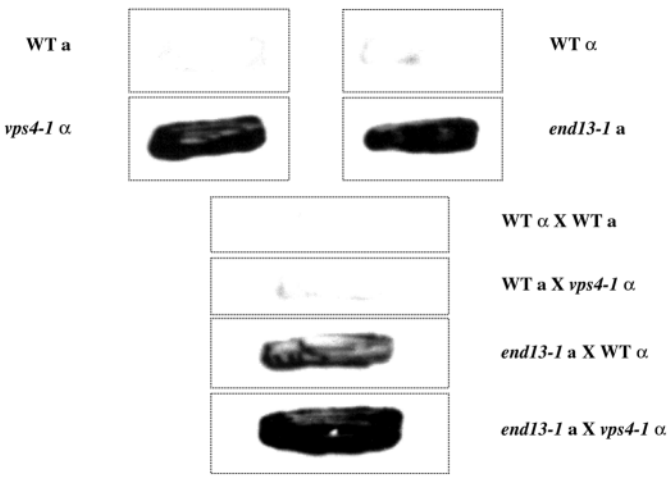

Fig. 1. The vacuolar protein sorting defects of *end13-1* and *vps4-1* do not complement and *end13-1* is weakly dominant. WT=*END13*/*VPS4*. See text for details. *END13*/*END13* (RH978 × RH2635), *END13*/*end13-1* (RH2635 × RH2606), *vps4-1*/*END13* (SF838-1D *vps4-1* × RH978) and *vps4-1*/*end13-1* (SF838-1D *vps4-1* × RH2606) diploid strains as well as *END13* (RH978 and RH2635), *end13-1* (RH2606) and *vps4-1* (SF838-1D *vps4-1*) parental haploid strains were grown at 24°C on YPUAD solid medium for 2 days in contact with a nitrocellulose filter. The filter was removed, the cells were eluted, and the filter was tested for secreted CPY by immunoblotting with a polyclonal CPY-specific antiserum.

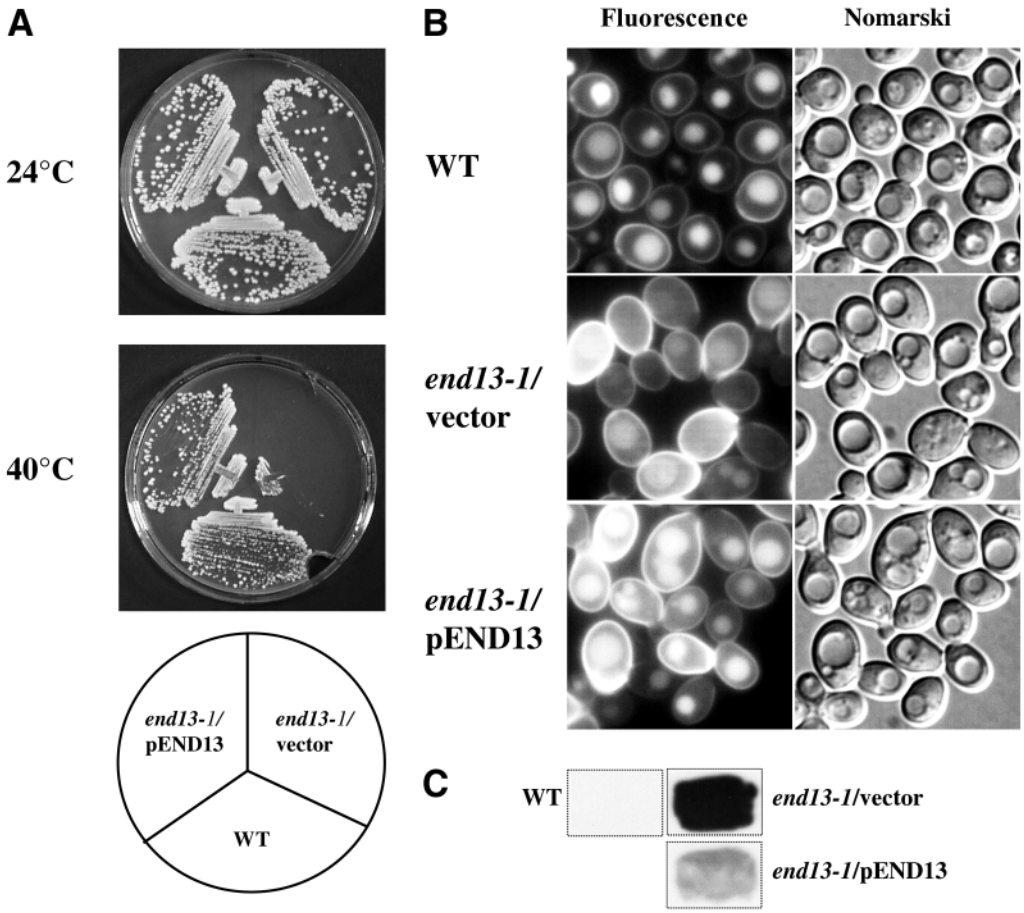

Fig. 2. Complementation of *end13-1* by the wild-type *END13* gene on a centromere plasmid. **(**A) An *end13-1* (RH2604) mutant strain was transformed with a centromere-based plasmid, pEND13.1, containing wild-type *END13* (pEND13) or with the YCplac111 vector alone (vector) and both transformed strains and a wild-type strain (RH1800) were tested for colony formation on YPUAD solid medium after 4 days at 24°C or 40°C. (B) The same strains were assayed for fluid-phase endocytosis of LY at 30°C. The same field of cells was observed by Nomarski optics (right) to visualise vacuoles (which appear as indentations in the cell profiles) or by fluorescein isothiocyanate fluorescence optics (left) to visualise LY. (C) The same strains were assayed for secretion of CPY using the filter assay described in the legend to Fig. 1.

yield a heterozygous *end13Δ*/*END13* diploid (RH2905). Tetrad dissection of RH2905 and spore germination at 30°C on YPUAD yielded four viable colonies in each tetrad (data not shown), indicating that *end13Δ* haploid strains are viable at this temperature in our strain background. Like *end13-1*, *end13Δ* mutant strains formed colonies well on YPUAD at 24°C, but were unable to form colonies at 40°C (Fig. 4A). In contrast, our wild-type strain formed colonies well at 24°C and more slowly at 40°C.

To examine the effect of loss of End13p on fluid-phase endocytosis, LY accumulation assays were carried out on wild-type (RH1800), as well as *end13Δ* (RH2906) strains carrying either a centromere-based plasmid containing the wild-type *END13* gene (pEND13.1) or vector (YCplac111) alone (Fig. 4B). *end13Δ* mutant cells showed significant defects in LY accumulation under these conditions compared to wild-type cells (RH1800) and the defect was complemented by the plasmid-borne *END13* gene. The *end13Δ* strain also had a vacuolar protein sorting defect, leading to secretion of CPY (Fig. 4C). This defect was also corrected by introduction of the *END13* gene on a centromeric plasmid.

^{35}S-α-factor uptake and transport to the vacuole at 30°C was also analysed in wild-type (RH1800), *end13-1* (RH2604), and *end13Δ* (RH2906) strains (Fig. 5). ^{35}S-α-factor was

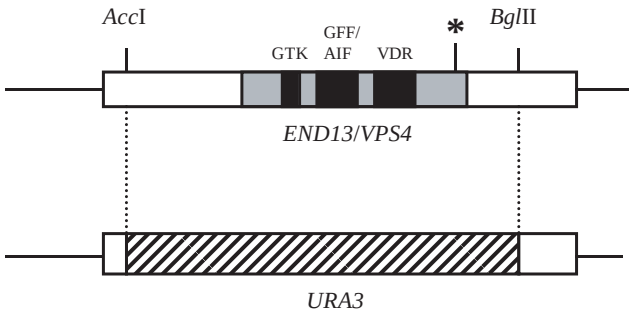

Fig. 3. Domain structure of End13p showing the site of the *end13-1* mutation and the size of the deletion in *end13Δ.* A schematic diagram of End13p showing the AAA-ATPase homology domain and the two motifs involved in ATP binding and hydrolysis (GTK and GFF/AIF), the motif involved in protein conformational changes induced by ATP binding (VDR), the position of the serine 335 to phenylalanine mutation in *end13-1* (asterisk), and the size of the deletion in *end13Δ* (below).

internalised with rapid kinetics in all three strains under these conditions (note rapid appearance of pH 1-resistant radioactive spots). In the *end13-1* and *end13Δ* mutant strains, however, vacuolar delivery of the internalised ^{35}S-α-factor (as measured by loss of intact ^{35}S-α-factor spots and appearance of degraded ^{35}S-α-factor spots) is inefficient compared to the wild-type strain.

End13p is required for efficient transport from early to late endosomes

To investigate where the delay in endocytic membrane transport occurs in *end13-1* mutant cells, we analysed internalisation and vacuolar delivery of the fluorescent lipid-soluble styryl dye FM4-64 (Vida and Emr, 1995) in wild-type and *end13-1* cells (Fig. 6). After incubation of *end13-1* mutant cells with FM4-64 for 20 minutes at 15°C and without chase, we observed punctate labelling at the cell periphery characteristic of early endosomes. The FM4-64 still localised mainly to these early endosomes after the cells were washed at 0°C and even after 5 minutes incubation at 30°C in fresh medium. Following subsequent incubation at 30°C the FM4-64 was gradually transported out of the peripheral early endosomes and after 30 minutes FM4-64 predominantly labelled a single large structure adjacent to the vacuole (class E compartment), similar to what has previously been reported for other *end13* mutants (Odorizzi et al., 1998). The vacuolar membrane was also labelled, but more weakly than in wild-type cells. In wild-type cells we observed punctate staining after incubation with FM4-64 for 20 minutes at 15°C, both before and after the wash (Fig. 6). After incubation at 30°C for 5 minutes, the FM4-64 predominantly labelled perivacuolar structures with the appearance of late endosomes as well as the vacuolar membrane itself. The FM4-64 labelled only the vacuolar membrane after 10 minutes of incubation at 30°C.

We then investigated transport of internalised ^{35}S-α-factor through the various endocytic compartments using equilibrium density gradient fractionation. ^{35}S-α-factor was prebound to wild-type (RH1800) and *end13-1* mutant (RH2604) cells on ice and then chased through the endocytic pathway at 30°C for various times. At each time point, a sample of cells was lysed and an endosome-enriched fraction was subjected to density gradient fractionation to separate early and late endosomes (Singer and Riezman, 1990; Singer-Krüger et al., 1993). The relative amount of ^{35}S-α-factor in each gradient fraction was determined by radioactivity and plotted (Fig. 7A). In wild-type cells (*END13*) at the 0 minute time point there were two peaks of ^{35}S-α-factor. The peak labelled EE in Fig. 7A fractionates at the position described by Singer-Krüger et al. for the kinetically defined early endosome (Singer-Krüger et al., 1993). The peak labelled PM in Fig. 7A most likely corresponds to plasma membrane, as it cofractionates with plasma membrane H^+-ATPase and the plasma membrane protein Gas1p (our unpublished results). A third peak, corresponding to the late endosome (LE) (Singer-Krüger et al., 1993) appears after 5 minutes of chase. The LE

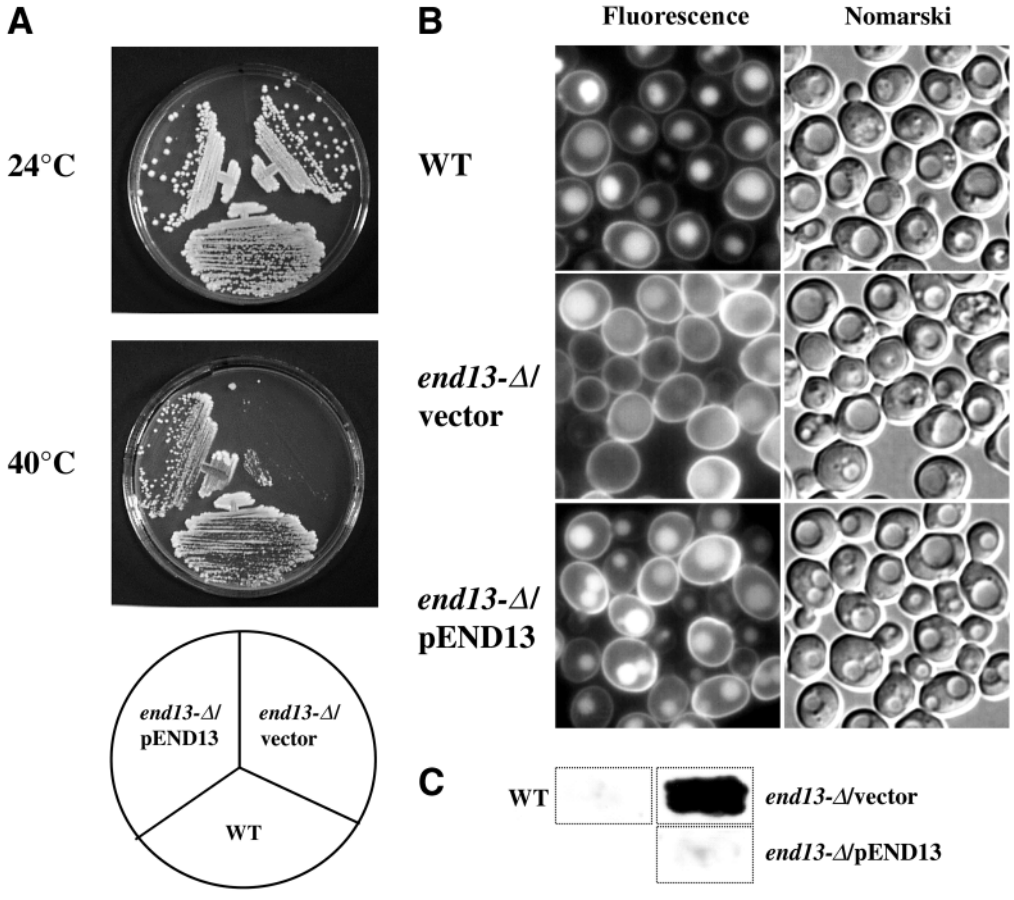

Fig. 4. End13p is required for growth at high temperature, fluid-phase endocytosis of LY and sorting of CPY to the vacuole. (A) An *end13Δ* (RH2906) mutant strain was transformed with a centromere-based plasmid, pEND13.1, containing wild-type *END13* (pEND13) or with the YCplac111 vector alone (vector), and both transformed strains and a wild-type strain (RH1800) were tested for colony formation on YPUAD solid medium after 4 days at 24°C or 40°C. (B) The same strains were assayed for fluid-phase endocytosis of LY at 30°C. The same field of cells was observed by Nomarski optics (right) to visualise vacuoles (which appear as indentations in the cell profiles) or by fluorescein isothiocyanate fluorescence optics (left) to visualise LY. (C) The same strains were assayed for secretion of CPY using the filter assay described in the legend to Fig. 1.

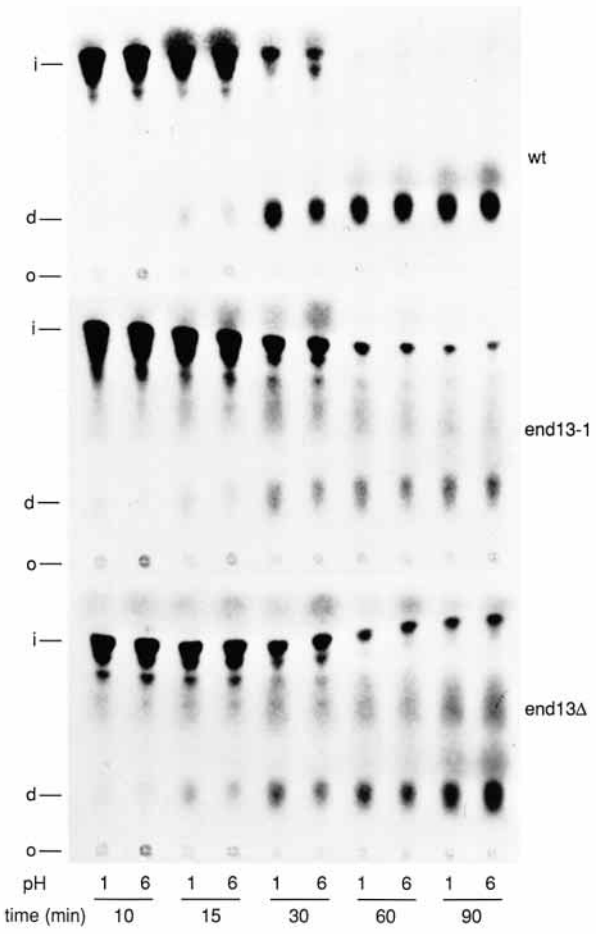

Fig. 5. Transport of internalised α-factor to the vacuole is delayed in *end13-1* and *end13Δ* mutant cells. Wild-type (RH1800), *end13-1* (RH2604) and *end13Δ* (RH2906) cells were grown to early exponential phase and assayed for ^{35}S-α-factor transport to the vacuole and degradation at 30°C. ^{35}S-α-factor was prebound to the cells on ice and then the cells were harvested at 4°C and resuspended in fresh YPUAD and incubated at 30°C. At the time points shown, duplicate samples were washed in either phosphate buffer pH 6 (removes unbound ^{35}S-α-factor) or citrate buffer pH 1 (removes surface, i.e. non-internalised, ^{35}S-α-factor). Cell lysates were prepared from each sample of cells and subjected to thin layer chromatography to separate intact (i) and degraded (d) ^{35}S-α-factor, which were visualised by fluorography at –80°C. o, origin where samples were loaded; 1, washed in pH 1 buffer; 6, washed in pH 6 buffer.

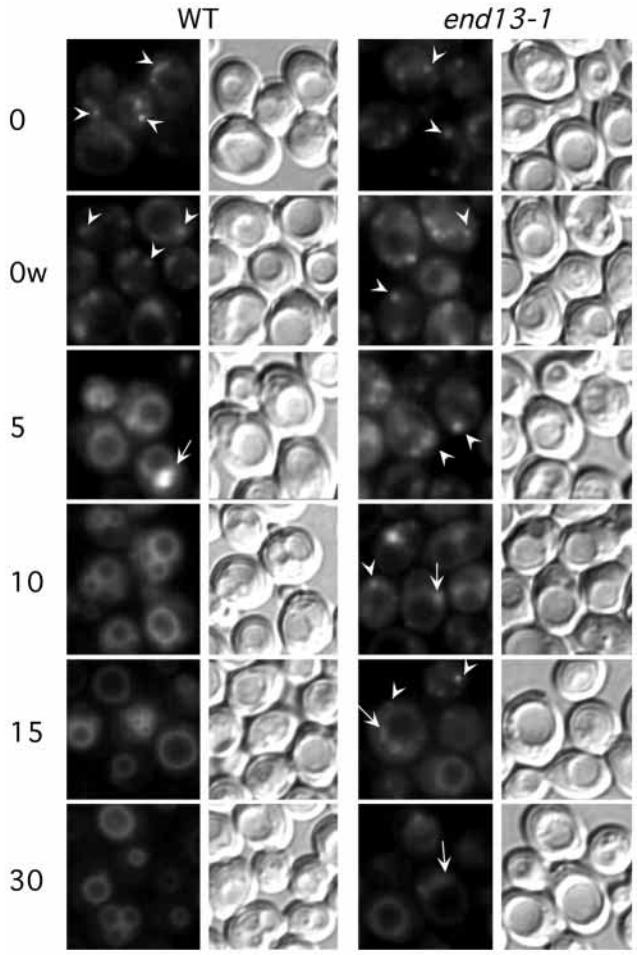

Fig. 6. Transport of FM4-64 in *end13-1* cells is delayed between early and late endosomes. Wild-type (WT) (RH1800) and *end13-1* (RH2604) cells were grown to early exponential phase and then incubated with FM4-64 at 15°C for 20 minutes. The cells were washed in ice-cold YPUAD and resuspended in YPUAD at 30°C without FM4-64. The cells were then incubated at 30°C. Samples of cells were taken after the 15°C incubation and before washing (0) or after washing (0w) and at 5, 10, 15 and 30 minutes after the shift to 30°C. Further membrane transport was stopped by chilling and addition of sodium azide and sodium fluoride. Cells were viewed by Texas Red-fluorescence optics to visualise FM4-64 (left panels) or by Nomarski optics to visualise vacuoles (appear as indentations; right panels). White arrowheads, early endosomes; white arrows, perivacuolar late endosomes.

peak grows at the expense of the EE peak by 15 minutes of chase. After 1 hour, the ^{35}S-α-factor has been chased out of the EE and LE peaks and is no longer in the endosome-enriched fraction. In the *end13-1* cells, the fractionation patterns of ^{35}S-α-factor at the 0 and 5 minute time points look quite similar to those seen in wild-type cells at these time points. At the 15 minute time point, however, it becomes obvious that ^{35}S-α-factor continues to accumulate in a compartment with a density characteristic of the early endosome, and does not appear in late endosomes. This result indicates a delay in transport between the early and late endosome. Transport is not completely blocked, however, because after 1 hour ^{35}S-α-factor is chased out of the endosomal compartments, similar to what was observed in wild-type cells. A similar, albeit not quite as pronounced, transport delay between early and late endosomes was seen in *end13Δ* cells (RH2906) (our unpublished results).

In order to investigate more closely the transport delay in *end13-1* cells, we looked at the time window between 15 and 60 minutes after shift to 30°C. As can be seen in Fig. 7B, in wild-type cells ^{35}S-α-factor has already been largely chased through both early and late endosomes after 30 minutes. In contrast, in the *end13-1* cells, a substantial ^{35}S-α-factor peak remains at the position of the early endosome after 30 minutes. To illustrate this point, we have plotted the kinetics of ^{35}S-α-factor transport out of the EE peak in Fig. 7C. From this data

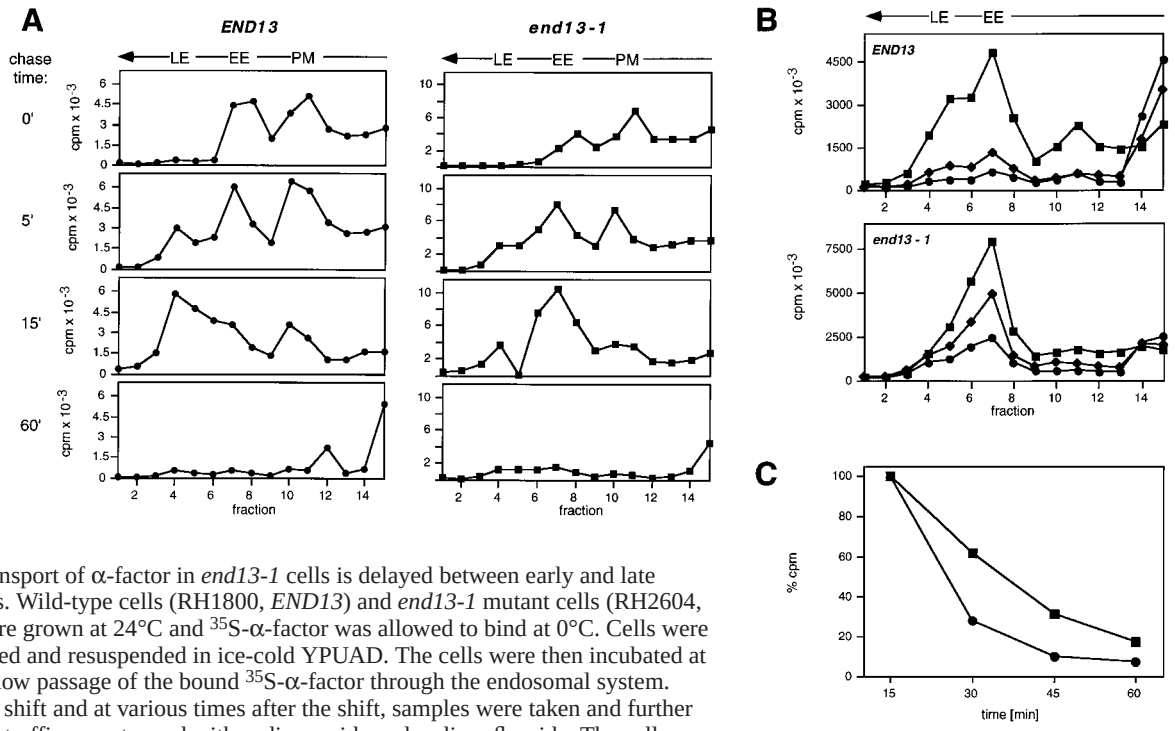

Fig. 7. Transport of α-factor in *end13-1* cells is delayed between early and late endosomes. Wild-type cells (RH1800, *END13*) and *end13-1* mutant cells (RH2604, *end13*) were grown at 24°C and ^{35}S-α-factor was allowed to bind at 0°C. Cells were then pelleted and resuspended in ice-cold YPUAD. The cells were then incubated at 30°C to allow passage of the bound ^{35}S-α-factor through the endosomal system. Before the shift and at various times after the shift, samples were taken and further membrane traffic was stopped with sodium azide and sodium fluoride. The cells were treated with lyticase and lysed by osmotic shock. After centrifugation at 7,500 ***g*** for 5 minutes, endosomal membrane material in the supernatant was pelleted at 128,000 ***g*** in an ultracentrifuge. The pellet was resuspended, transferred into a new tube, overlayed with a Nycodenz step gradient and membranes were floated to equilibrium density by ultracentrifugation. The gradients were fractionated from the top into 15 fractions which were counted in a scintillation counter. (A) Gradient profile of ^{35}S-α-factor counts from wild-type (*END13*) and *end13-1* cells with increasing chase times (minutes). Arrows indicate the direction of membrane flotation. PM, plasma membrane; EE, early endosome; LE, late endosome. (B) Gradient profile of ^{35}S-α-factor counts from wild-type (*END13*) and *end13-1* (*end13*) cells with increasing chase times: squares, 15 minutes; diamonds, 30 minutes; circles, 45 minutes. Arrow indicates direction of membrane flotation. EE, early endosome; LE, late endosome. (C) Time course of relative ^{35}S-α-factor counts in the early endosome peak fraction #7 from the experiment shown in B (gradient profile for 60 minute time point is not shown in B). Circles, wild-type; squares, *end13-1*. The counts in fraction #7 after 15 minutes of chase were set at 100%.

an approximate apparent $t_{1/2}$ of 25 minutes for early endosome exit in wild-type cells can be derived, whereas in *end13-1* cells the apparent $t_{1/2}$ for early endosome exit is approximately 36 minutes.

end13 mutants have been reported to be defective in transport between the late endosome/PVC and the vacuole and to accumulate enlarged late endosomes/PVCs (Babst et al., 1998; Odorizzi et al., 1998). Since we did not see a marked accumulation of ^{35}S-α-factor in a compartment with the characteristic density of late endosomes in our density gradient analysis of P2 from *end13-1* cells, we considered the possibility that the late endosomes may have been enlarged in the *end13-1* cells and thus have been efficiently removed in P1. To test this, we followed the distribution of late endosomes during our density gradient fractionation using CPY as a marker. P2 fractions were obtained from wild-type (RH1800) and *end13-1* (RH2604) cells and these were then subjected to analysis on the same density gradients used to analyse ^{35}S-α-factor distribution (Fig. 8). We found that the P2 of *end13-1* cells contained significantly less CPY than the P2 of wild-type cells (data not shown). In density gradients, the CPY present in the P2 of wild-type cells predominantly migrated in a single peak with a density characteristic of late endosomes (peak at fraction 5). A minor peak of CPY exhibited a density characteristic of early endosomes (peak at fraction 8), and another minor peak was more dense and may represent a late Golgi compartment (peak at fraction 15). In contrast, when the P2 of *end13-1* cells was analysed, fractions 4-6 contained much less CPY than seen in wild-type and the peak fraction (4) contained no more CPY than the early endosome peak fraction (7). This result supports the conclusion that late endosomes may have been depleted from the P2 of *end13-1* cells relative to the P2 of wild-type cells. Although vacuoles containing mature CPY would have been removed in P1, most of the CPY in the endosome-enriched P2 was not the size of the p2 CPY precursor (69 kDa), but rather the size of mature CPY (61 kDa). This may be due to proteolysis of the p2 CPY within endosomes during the lengthy centrifugation steps. The use of protease inhibitors did not prevent this proteolysis.

We then used immunofluorescence detection to follow Ste2p (α-factor receptor) internalisation and transport through the endosomal pathway morphologically. Wild-type (RH1800), *end13-1* (RH2604) and *end13Δ* (RH2906) cells were treated with cycloheximide to prevent further Ste2p synthesis and to chase existing Ste2p molecules in the secretory pathway to the cell surface. Then synthetic α-factor peptide was added to the cells for different times at 30°C to induce Ste2p internalisation and transport to the vacuole. At different time points after α-factor addition, samples of cells were taken, fixed and stained with Ste2p-specific antiserum

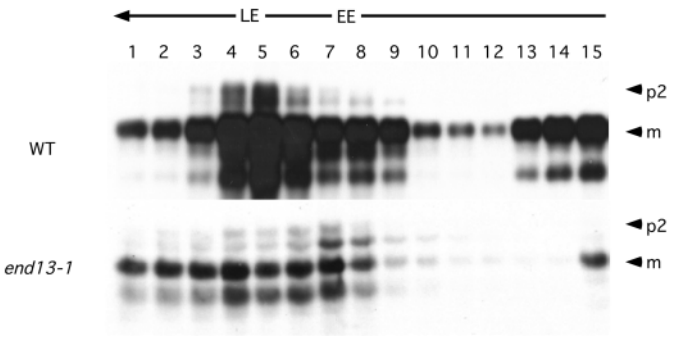

Fig. 8. Gradient profile of CPY present in the P2 fraction from wild-type and *end13-1* cells. Wild-type cells (RH1800, WT) and *end13-1* mutant cells (RH2604) were grown at 24°C to 1×10^7 cells/ml and 250 OD_{600} units were harvested. The cells were spheroplasted with Zymolyase 20T and lysed by osmotic shock. Unlysed cells were removed at 300 ***g*** for 5 minutes. The lysate was then subjected to centrifugation at 7500 ***g*** for 5 minutes to yield pellet P1 and supernatant S1. Endosomal membrane material in the S1 was pelleted at 128,000 ***g*** in an ultracentrifuge to yield pellet P2. P2 was resuspended, transferred into a new tube, overlayed with a Nycodenz step gradient and membranes were floated to equilibrium density by ultracentrifugation as in Fig. 7. The gradients were fractionated into 15 fractions from the top as in Fig. 7. Each fraction was analysed by SDS-PAGE followed by transfer to a PVDF membrane and immune detection of CPY with a specific monoclonal antiserum. Note that 10% of the wild-type fractions and 40% of the *end13-1* fractions were analysed. The arrow at the top of the panel indicates the direction of membrane flotation. Numbers 1-15 are fraction numbers. EE, early endosome peak fraction (from Fig. 7A); LE, late endosome peak fraction (from Fig. 7A). Arrowheads indicate position of p2CPY (p2) and mature CPY (m).

(Fig. 9). In wild-type cells, Ste2p clears rapidly from the cell surface as indicated by the loss of diffuse surface staining and the increase in staining of a large number of small punctate structures at the cell periphery. The appearance and localisation of these compartments is characteristic of early endosomes (Hicke et al., 1997). At later time points, Ste2p reaches larger and less numerous punctate structures within the cell and often near the vacuole. The appearance and localisation of these compartments is typical of late endosomes (Hicke et al., 1997). In contrast, in both *end13-1* and *end13Δ* mutant cells, while Ste2p clears rapidly from the cell surface, delivery from small peripheral early endosomes to late endosomes is markedly delayed. Eventually, however, Ste2p does appear in late endosomes. We were not able to follow subsequent Ste2p transport from late endosomes to the vacuole in this experiment, because cycloheximide inhibits this transport step (Hicke et al., 1997) and furthermore, any Ste2p that reaches the vacuole will be rapidly degraded by vacuolar proteases.

DISCUSSION

We show here that the *END13* gene, identified as a *vma2*(*vat2*)*Δ* synthetic lethal mutant with post-internalisation defects in the endocytic pathway (Munn and Riezman, 1994; Riezman et al., 1996), is identical to the class E vacuolar protein sorting gene *VPS4* (Babst et al., 1997) and encodes an AAA-family ATPase. Consistent with *end13-1* being allelic to *vps4*, *end13-1* does not complement the vacuolar protein sorting defect of a *vps4-1* (previously known as *vpl4-1*) mutant (Rothman and Stevens, 1986; Rothman et al., 1989; Raymond et al., 1992) (Fig. 1). Furthermore, we determined that *end13-1* is an S335F mutation in the conserved AAA-ATPase domain of End13p/Vps4p (Fig. 3).

Disruption of *END13* in our strain background led to phenotypes similar to *end13-1*. Like *end13-1*, *end13Δ* mutants are temperature-sensitive for growth, growing poorly at 37°C and unable to form colonies at 40°C (Figs 2A, 4A). This temperature-sensitive growth defect is quite common in mutants lacking proteins involved in endocytosis, but the physiological basis for this conditional growth defect is not understood (Bénédetti et al., 1994; Munn and Riezman, 1994; Munn et al., 1995; Wesp et al., 1997; Naqvi et al., 1998; Munn, 2000). *end13Δ* mutants are also defective in LY accumulation in the vacuole and in transport of internalised α-factor to the vacuole at all temperatures, like the original *end13-1* mutant (Munn and Riezman, 1994) (Figs 2B, 4B, 5).

We investigated using both biochemical fractionation and fluorescence microscopy approaches where End13p is required in the endocytic pathway to the vacuole. Our results from FM4-64 internalisation assays (Fig. 6), biochemical fractionation experiments (Fig. 7) and Ste2p immunofluorescence localisations (Fig. 9) show that in *end13* mutant cells there is a strong delay in transport of FM4-64, α-factor and Ste2p from early to late endosomes.

Although a number of mutations have been characterised in End13p, the mutation in *end13-1* is novel. It lies within the AAA-ATPase homology domain of the protein, which extends from residues 229 to 350 (Babst et al., 1997; Finken-Eigen et al., 1997). There are three motifs within this AAA-ATPase homology domain that define this domain and which are likely to be involved in ATP binding, ATP hydrolysis or ATP-dependent conformational changes of the protein (GTK/Walker box A, GFF/Walker box B, and VDR motifs, respectively). Site-directed mutagenesis studies have shown that a K179A substitution in the GTK motif or an E233Q substitution within the GFF motif of this domain can abolish function (Babst et al., 1997). Other mutations within the AAA-ATPase domain of End13p were identified in screens for dominant negative *vps* mutants. Three dominant negative mutations were identified: E211K (in GFF motif), G178D (in GTK motif), as well as E233Q (same as the mutation made by Babst et al., 1997 in the GFF motif) (Finken-Eigen et al., 1997). The mutation in *end13-1*, in contrast, maps outside the three motifs involved in ATP binding and hydrolysis, but still within the region of homology shared by all AAA-family ATPases. The *end13-1* mutation is only partially dominant, unlike mutations in the GTK and GFF motifs, which are fully dominant. S335 lies within a GYSG motif, which is completely conserved in the AAA-homology domain of End13p homologues from human, mouse and *Schizosaccharomyces pombe* (Babst et al., 1997). A temperature-sensitive-for-function mutant (*vps4-ts*) has been reported to have two mutations in a similar region of the AAA-ATPase homology region, M307T and L327S (Babst et al., 1997) and these two mutations also affect residues completely conserved in all known End13p homologues.

Work from several laboratories has shown that End13p acts

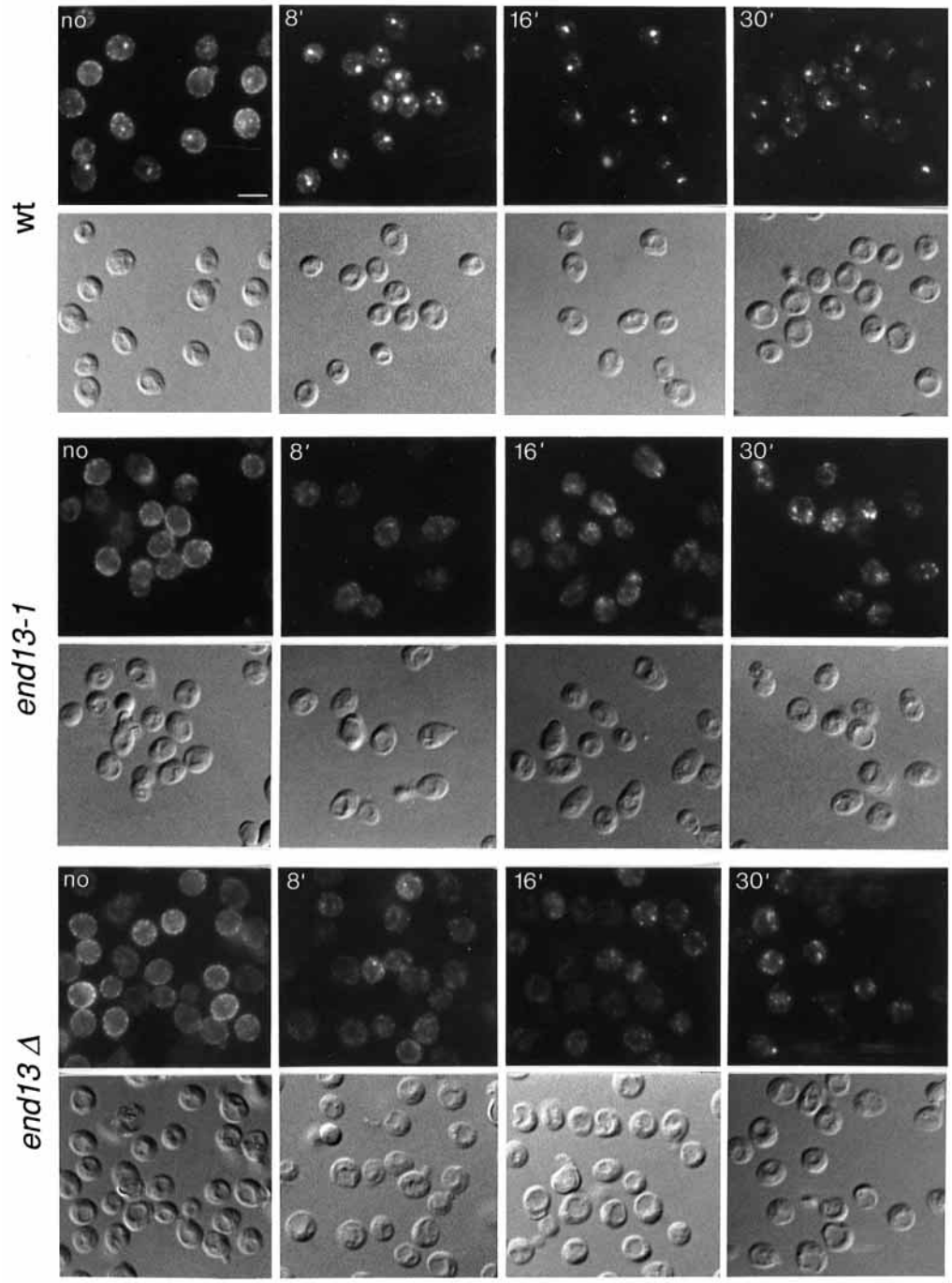

Fig. 9. Transport of Ste2p in *end13-1* and *end13Δ* cells is delayed between early and late endosomes. Wild-type (wt; RH1800), *end13-1* (RH2604) and *end13Δ* (RH2906) cells were grown to early exponential phase at 24°C, harvested, resuspended to 1×10^7 cells/ml in YPUAD, and treated for 10 minutes with 20 μg/ml cycloheximide at 30°C to inhibit new Ste2p synthesis and to chase existing Ste2p to the cell surface. Then 10^{-7} M synthetic α-factor was added to the culture and the cells were incubated at 30°C to induce Ste2p internalisation and transport to the vacuole. Before α-factor addition (no) and 8, 16 and 30 minutes after α-factor addition, samples of cells were taken, fixed, attached to microscope slides and stained with a rabbit polyclonal anti-Ste2p antiserum followed by Cy3-conjugated goat anti-rabbit IgG. Stained cells were visualised by Nomarski (lower panels) and rhodamine-fluorescence optics (upper panels) to visualise cells and Ste2p, respectively. Scale bar, 5 μm.

in biosynthetic membrane transport from the PVC/late endosome to the vacuole and that mutations in *END13* are associated with the accumulation of aberrant 'class E *vps*' PVCs adjacent to the vacuole (Rothman and Stevens, 1986; Munn and Riezman, 1994; Babst et al., 1997; Finken-Eigen et al., 1997; Odorizzi et al., 1998; Babst et al., 1998). Class E compartments accumulate in a number of *vps* mutants (so-called 'class E' *vps* mutants) and have been shown to contain newly synthesised vacuolar proteins, internalised plasma membrane proteins, and resident proteins of the trans-Golgi Network (TGN) (Davis et al., 1993; Cereghino et al., 1995; Piper et al., 1995; Rieder et al., 1996; Babst et al., 1998; Odorizzi et al., 1998). In class E *vps* mutants there is likely to be a block in both forward transport from the defective class E compartment to the vacuole, as well as in recycling of proteins from the defective class E compartment back to the TGN (reviewed in Bryant and Stevens, 1998; Munn, 2000).

In contrast to these previous reports regarding other *end13* alleles, we have demonstrated here a defect in endosomal transport between early endosomes and late endosomes in *end13-1* mutants. This defect is not specific to the *end13-1* allele because the *end13Δ* mutant also shows a defect in early to late endosome transport. We could not see any accumulation of ^{35}S-α-factor in any compartments except early endosomes in our fractionation experiments. We cannot formally exclude, however, accumulation in late endosomes if these were

enlarged in *end13* mutants to the point where they were removed in the low speed (P1) pellet along with vacuoles and therefore not been present in the endosome-enriched P2 fraction loaded onto the equilibrium density gradients. In support of this possibility, we found significantly less CPY in the P2 of *end13-1* cells compared with the P2 of wild-type cells (data not shown). This was observed even though *end13-1*, like other *end13* alleles, causes a defect in transport of CPY through late endosomes to the vacuole and would be predicted to accumulate CPY in late endosomes (Munn and Riezman, 1994; this study). Moreover, CPY in the wild-type P2 migrated on equilibrium density gradients in a major peak at a density characteristic of late endosomes, while the residual CPY in the *end13-1* P2 did not form a major peak at this density. Because of this apparent loss of late endosomes from the *end13-1* P2, we are unable to conclude whether ^{35}S-α-factor accumulates in late endosomes and whether ^{35}S-α-factor transport from late endosomes to vacuoles was delayed in *end13-1* cells. Our experiments, however, clearly demonstrate a novel role for End13p in early to late endosome transport.

From our experiments it is not possible to determine whether the defect in transport from early endosomes to late endosomes is a direct or indirect effect of loss of End13p function since both *end13-1* and *end13Δ* cells had grown for extensive periods without functional End13p. We attempted to resolve this question by testing the temperature-sensitive-for-function allele mentioned above (*vps4-ts* with mutations M307T and L327S) in which End13p is fully functional at 24°C but becomes immediately defective for CPY delivery to the vacuole after shift to 37°C (Babst et al., 1997). Unexpectedly, however, when introduced on a centromeric plasmid into *end13Δ*, this *vps4-ts* allele fully complemented the defects in both LY accumulation in the vacuole and Ste2p transport through early endosomes at 37°C. These endocytic functions were restored by *vps4-ts*, even when assayed after extensive (30 minute) preincubation at 37°C (data not shown). Nevertheless, this *vps4-ts* plasmid did not correct the strong temperature-sensitive growth defect of *end13Δ* on solid medium (data not shown). Furthermore, secretion of CPY by *end13Δ* was corrected at 24°C, but not at 37°C, by plasmid-borne *vps4-ts* (data not shown). This suggests that End13p may have more than one function and that the *vps4-ts* allele affects CPY transport to the vacuole more than Ste2p transport through early endosomes or LY delivery to the vacuole.

Earlier studies did not reveal defects in early to late endosome transport in mutants lacking End13p; however, a full kinetic analysis was not presented in these reports and it is possible that a delay in early to late endosome transport was overlooked (Babst et al., 1997; Finken-Eigen et al., 1997; Babst et al., 1998; Odorizzi et al., 1998). We do see labelling of a compartment resembling the 'class E compartment' adjacent to the vacuole with FM4-64 in *end13-1* cells after 30 minutes of chase at 30°C, as previously reported by Odorizzi et al. (Odorizzi et al., 1998); however, there is clearly a defect in prior transport of the dye through earlier endocytic compartments. Interestingly, the early endosomes in *end13Δ* mutant cells are not defective for all membrane transport events, since it has been recently reported that membrane recycling to the plasma membrane can occur normally from the early endosomes in these mutants (Wiederkehr et al., 2000). This suggests that a specific transport step out of the early endosome is affected by loss of End13p and that the early endosome retains some function in *end13* mutants. This may explain why the early endosomes do not appear significantly enlarged in *end13-1* mutant cells.

A role for End13p in early to late endosome transport in yeast is supported by a recent study on the mouse homologue of End13p (SKD1) (Yoshimori et al., 2000). A dominant negative mutant form of SKD1 (E235Q, equivalent to End13p E233Q) was expressed in tissue culture cells and the effects on the endocytic pathway were examined. Overexpression of the SKD1(E235Q) caused the appearance of abnormal endosomes which contain both endocytosed fluid and receptors, as well as lysosomal markers. Expression of SKD1(E235Q) also blocked lysosomal degradation of internalised epidermal growth factor receptors. The aberrant endosomes induced by SKD1(E235Q) expression label with antiserum to EEA1, an early endosome-specific marker, but do not contain late endosomal markers, indicating that they are of early endosomal origin. On the other hand, the cellular localisation and morphology of these aberrant endosomes (perinuclear) was similar to that of late endosomes. In addition, Bishop and Woodman (Bishop and Woodman, 2000) have shown that ATPase-deficient mutants (K168Q and E223Q) of a human End13p homologue (hVps4p) bind both early and late endosomes in transfected tissue culture cells and alter both early and late endosomal morphology, although in this study the function of these aberrant compartments was not analysed.

End13p is required for the formation of the internal vesicles present in multivesicular (i.e. late) endosomes/PVCs (Odorizzi et al., 1998). Is a function for End13p in early endosomes consistent with a role in formation of the internal vesicles within late endosomes? Indeed, in mammalian cells transferrin-receptor positive early endosomes do contain some internal vesicles (albeit less numerous than late endosomes) (Hopkins et al., 1990; Futter et al., 1996). Internal vesicles have

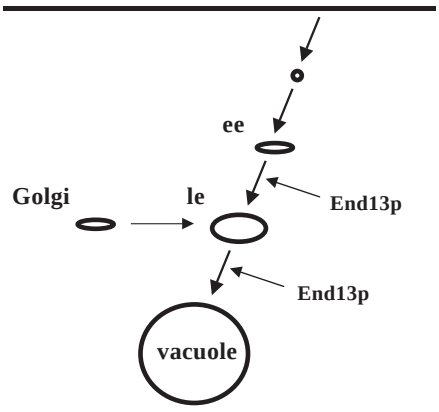

Fig. 10. End13p functions in multiple membrane transport steps in the yeast endocytic pathway. A schematic diagram indicating the endocytic membrane transport steps in which End13p is proposed to function. For the biosynthetic transport pathway to the vacuole, the defect in late endosome (le) to vacuole transport in *end13* mutants leads to transient accumulation of vacuolar precursors in the late endosome. In the endocytic transport pathway of FM4-64 and Ste2p from the cell surface to the vacuole, the defect in early endosome (ee) to late endosome (le) transport leads to transient accumulation of these endocytic markers in early endosomes.

been visualised in late endosomes in yeast (Prescianotto-Baschong and Riezman, 1998; Mulholland et al., 1999). While internal vesicles have not yet been reported in early endosomes of yeast cells, it is possible that the process of internal vesicle formation initiates in early endosomes in yeast as well as in mammals (see Munn, 2000). So we believe that End13p may function in both early and late endosomes to form internal vesicles and to facilitate transport through these compartments.

The primary role of End13p in biosynthetic transport of proteins such as CPY and proteinase A to the vacuole may be in transport from the PVC to the vacuole (Babst et al., 1997; Finken-Eigen et al., 1997; Odorizzi et al., 1998; Babst et al., 1998). In contrast, efficient transport of Ste2p from the cell surface to the vacuole through the endocytic pathway, as investigated here, clearly requires End13p function in early endosomes. Our data show that *end13* mutants have defects in multiple steps of the endocytic pathway, as depicted in Fig. 10. This endocytic membrane traffic phenotype is somewhat reminiscent of the multiple membrane traffic defects associated with *sec18* mutations. *sec18* mutants are defective in another AAA-ATPase, Sec18p/NEM-sensitive fusion protein (NSF), and have defects in multiple steps of the secretory and endocytic pathways (Graham and Emr, 1991; Haas and Wickner, 1996; Mayer et al., 1996; Hicke et al., 1997).

We thank F. Cvrckova for sending the YCplac111 *S. cerevisiae* genomic library and T. Stevens for sending the *vps* mutant collection. This work was made possible by funding from the National Science and Technology Board of Singapore to A.M. and from the Kanton Baselstadt and Swiss National Science Foundation to H.R.

REFERENCES

Adams, A., Gottschling, D. E., Kaiser, K. A. and Stearns, T. (1997). *Methods in Yeast Genetics. A Cold Spring Harbor Laboratory Course Manual*. Cold Spring Harbor, New York: Cold Spring Harbor Laboratory Press.

Babst, M., Sato, T. K., Banta, L. M. and Emr, S. D. (1997). Endosomal transport function in yeast requires a novel AAA-type ATPase, Vps4p. *EMBO J.* **16**, 1820-1831.

Babst, M., Wendland, B., Estepa, E. J. and Emr, S. D. (1998). The Vps4p AAA ATPase regulates membrane association of a Vps protein complex required for normal endosome function. *EMBO J.* **17**, 2982-2993.

Bankaitis, V. A., Johnson, L. M. and Emr, S. D. (1986). Isolation of yeast mutants defective in protein targeting to the vacuole. *Proc. Natl. Acad. Sci. USA* **83**, 9075-9079.

Banta, L. M., Robinson, J. S., Klionsky, D. J. and Emr, S. D. (1988). Organelle assembly in yeast: characterization of yeast mutants defective in vacuolar biogenesis and protein sorting. *J. Cell Biol.* **107**, 1369-1383.

Bénédetti, H., Raths, S., Crausaz, F. and Riezman, H. (1994). The *END3* gene encodes a protein that is required for the internalization step of endocytosis and for actin cytoskeleton organization in yeast. *Mol. Biol. Cell* **5**, 1023-1037.

Bishop, N. and Woodman, P. (2000). ATPase-defective mammalian *VPS4* localizes to aberrant endosomes and impairs cholesterol trafficking. *Mol. Biol. Cell* **11**, 227-239.

Botstein, D., Falco, S. C., Stewart, S. E., Brennan, M., Scherer, S., Stinchcomb, D. T., Struhl, K. and Davis, R. W. (1979). Sterile host yeasts (SHY): a eukaryotic system of biological containment for recombinant DNA experiments. *Gene* **8**, 17-24.

Bryant, N. J. and Stevens, T. H. (1998). Vacuole biogenesis in *Saccharomyces cerevisiae*: protein transport pathways to the yeast vacuole. *Microbiol. Mol. Biol. Rev.* **62**, 230-247.

Cereghino, J. L., Marcusson, E. G. and Emr, S. D. (1995). The cytoplasmic tail domain of the vacuolar protein sorting receptor Vps10p and a subset of *VPS* gene products regulate receptor stability, function, and localization. *Mol. Biol. Cell* **6**, 1089-1102.

Davis, N. G., Horecka, J. L. and Sprague, G. F. Jr. (1993). Cis- and trans-acting functions required for endocytosis of the yeast pheromone receptors. *J. Cell Biol.* **122**, 53-65.

Dulic, V., Egerton, M., Elguindi, I., Raths, S., Singer, B. and Riezman, H. (1991). Yeast endocytosis assays. *Methods Enzymol.* **194**, 697-710.

Finken-Eigen, M., Rohricht, R. A. and Kohrer, K. (1997). The *VPS4* gene is involved in protein transport out of a yeast prevacuolar endosome-like compartment. *Curr. Genet.* **31**, 469-480.

Futter, C. E., Pearse, A., Hewlett, L. J. and Hopkins, C. R. (1996). Multivesicular endosomes containing internalized EGF-EGF receptor complexes mature and then fuse directly with lysosomes. *J. Cell Biol.* **132**, 1011-1023.

Gietz, R. D. and Sugino, A. (1988). New yeast-*Escherichia coli* shuttle vectors constructed with *in vitro* mutagenized yeast genes lacking six-base pair restriction sites. *Gene* **74**, 527-534.

Graham, T. R. and Emr, S. D. (1991). Compartmental organization of Golgi-specific protein modification and vacuolar protein sorting events defined in a yeast *sec18* (NSF) mutant. *J. Cell Biol.* **114**, 207-218.

Haas, A. and Wickner, W. (1996). Homotypic vacuole fusion requires Sec17p (yeast α-SNAP) and Sec18p (yeast NSF). *EMBO J.* **15**, 3296-3305.

Hicke, L. and Riezman, H. (1996). Ubiquitination of a yeast plasma membrane receptor signals its ligand-stimulated endocytosis. *Cell* **84**, 277-287.

Hicke, L., Zanolari, B., Pypaert, M., Rohrer, J. and Riezman, H. (1997). Transport through the yeast endocytic pathway occurs through morphologically distinct compartments and requires an active secretory pathway and Sec18p/N-ethylmaleimide-sensitive fusion protein. *Mol. Biol. Cell* **8**, 13-31.

Hopkins, C. R., Gibson, A., Shipman, M. and Miller, K. (1990). Movement of internalized ligand-receptor complexes along a continuous endosomal reticulum. *Nature* **346**, 335-339.

Klionsky, D. J., Herman, P. K. and Emr, S. D. (1990). The fungal vacuole: composition, function, and biogenesis. *Microbiol. Rev.* **54**, 266-292.

Mayer, A., Wickner, W. and Haas, A. (1996). Sec18p (NSF)-driven release of Sec17p (α-SNAP) can precede docking and fusion of yeast vacuoles. *Cell* **85**, 83-94.

Mulholland, J., Konopka, J., Singer-Krüger, B., Zerial, M. and Botstein, D. (1999). Visualization of receptor-mediated endocytosis in yeast. *Mol. Biol. Cell* **10**, 799-817.

Munn, A. L. (2000). The yeast endocytic membrane transport system. *Microsc. Res. Tech.* **51**, 547-562.

Munn, A. L. and Riezman, H. (1994). Endocytosis is required for the growth of vacuolar H^+-ATPase-defective yeast: identification of six new *END* genes. *J. Cell Biol.* **127**, 373-386.

Munn, A. L., Stevenson, B. J., Geli, M. I. and Riezman, H. (1995). *end5*, *end6*, and *end7*: mutations that cause actin delocalization and block the internalization step of endocytosis in *Saccharomyces cerevisiae*. *Mol. Biol. Cell* **6**, 1721-1742.

Munn, A. L., Heese-Peck, A., Stevenson, B. J., Pichler, H. and Riezman, H. (1999). Specific sterols required for the internalization step of endocytosis in yeast. *Mol. Biol. Cell* **10**, 3943-3957.

Naqvi, S. N., Zahn, R., Mitchell, D. A., Stevenson, B. J. and Munn, A. L. (1998). The WASp homologue Las17p functions with the WIP homologue End5p/verprolin and is essential for endocytosis in yeast. *Curr. Biol.* **8**, 959-962.

Odorizzi, G., Babst, M. and Emr, S. D. (1998). Fab1p PtdIns(3)P 5-kinase function essential for protein sorting in the multivesicular body. *Cell* **95**, 847-858.

Piper, R. C., Cooper, A. A., Yang, H. and Stevens, T. H. (1995). *VPS27* controls vacuolar and endocytic traffic through a prevacuolar compartment in *Saccharomyces cerevisiae*. *J. Cell Biol.* **131**, 603-617.

Prescianotto-Baschong, C. and Riezman, H. (1998). Morphology of the yeast endocytic pathway. *Mol. Biol. Cell* **9**, 173-189.

Raymond, C. K., Howald-Stevenson, I., Vater, C. A. and Stevens, T. H. (1992). Morphological classification of the yeast vacuolar protein sorting mutants: evidence for a prevacuolar compartment in class E *vps* mutants. *Mol. Biol. Cell* **3**, 1389-1402.

Rieder, S. E., Banta, L. M., Kohrer, K., McCaffery, J. M. and Emr, S. D. (1996). Multilamellar endosome-like compartment accumulates in the yeast *vps28* vacuolar protein sorting mutant. *Mol. Biol. Cell* **7**, 985-999.

Riezman, H., Munn, A., Geli, M. I. and Hicke, L. (1996). Actin-, myosin- and ubiquitin-dependent endocytosis. *Experientia* **52**, 1033-1041.

Robinson, J. S., Klionsky, D. J., Banta, L. M. and Emr, S. D. (1988). Protein sorting in *Saccharomyces cerevisiae*: isolation of mutants defective in the delivery and processing of multiple vacuolar hydrolases. *Mol. Cell. Biol.* **8**, 4936-4948.

Rothman, J. H. and Stevens, T. H. (1986). Protein sorting in yeast: mutants defective in vacuole biogenesis mislocalize vacuolar proteins into the late secretory pathway. *Cell* **47**, 1041-1051.

Rothman, J. H., Hunter, C. P., Valls, L. A. and Stevens, T. H. (1986). Overproduction-induced mislocalization of a yeast vacuolar protein allows isolation of its structural gene. *Proc. Natl. Acad. Sci. USA* **83**, 3248-3252.

Rothman, J. H., Howald, I. and Stevens, T. H. (1989). Characterization of genes required for protein sorting and vacuolar function in the yeast *Saccharomyces cerevisiae*. *EMBO J.* **8**, 2057-2065.

Sambrook, J., Fritsch, E. F. and Maniatis, T. (1989). *Molecular Cloning: A Laboratory Manual*. 2nd edition. Cold Spring Harbor, New York: Cold Spring Harbor Laboratory Press.

Singer, B. and Riezman, H. (1990). Detection of an intermediate compartment involved in transport of α-factor from the plasma membrane to the vacuole in yeast. *J. Cell Biol.* **110**, 1911-1922.

Singer-Krüger, B., Frank, R., Crausaz, F. and Riezman, H. (1993). Partial purification and characterization of early and late endosomes from yeast. Identification of four novel proteins. *J. Biol. Chem.* **268**, 14376-14386.

Stevens, T., Esmon, B. and Schekman, R. (1982). Early stages in the yeast secretory pathway are required for transport of carboxypeptidase Y to the vacuole. *Cell* **30**, 439-448.

Vida, T. A. and Emr, S. D. (1995). A new vital stain for visualizing vacuolar membrane dynamics and endocytosis in yeast. *J. Cell Biol.* **128**, 779-792.

Ward, A. C. (1990). Single-step purification of shuttle vectors from yeast for high frequency back-transformation into *E. coli*. *Nucl. Acid Res.* **18**, 5319.

Wesp, A., Hicke, L., Palecek, J., Lombardi, R., Aust, T., Munn, A. L. and Riezman, H. (1997). End4p/Sla2p interacts with actin-associated proteins for endocytosis in *Saccharomyces cerevisiae*. *Mol. Biol. Cell* **8**, 2291-2306.

Wiederkehr, A., Avaro, S., Prescianotto-Baschong, C., Haguenauer-Tsapis, R. and Riezman, H. (2000). The F-box protein Rcy1p is involved in endocytic membrane traffic and recycling out of an early endosome in *Saccharomyces cerevisiae*. *J. Cell Biol.* **149**, 397-410.

Yoshimori, T., Yamagata, F., Yamamoto, A., Mizushima, N., Kabeya, Y., Nara, A., Miwako, I., Ohashi, M., Ohsumi, M. and Ohsumi, Y. (2000). The mouse SKD1, a homologue of yeast Vps4p, is required for normal endosomal trafficking and morphology in mammalian cells. *Mol. Biol. Cell* **11**, 747-763.